ISABE-2009-1258

TURBULENCE MODEL COMPARISONS FOR A LOW PRESSURE 1.5 STAGE TEST TURBINE

Dwain Dunn and Glen Snedden
CSIR.
P.O. Box 395.
Pretoria 0001
South Africa

T.W. von Backström
Department of Mechanical Engineering,
University of Stellenbosch, 7600
South Africa

Abstract

In a gas turbine engine secondary flows have a detrimental effect on efficiency. The current numerical study is aimed at determining which turbulence model in a commercially available CFD code is best suited to predicting the secondary flows. Experimental validation is used to determine the appropriateness of the model. The numerical study was performed using Numeca's FINE^{TM}/Turbo and all of the appropriate turbulence models were tested. It was found that the Baldwin-Lomax, Spalart-Allmaras and *k*-ε predicted the magnitude of the velocity well, but did not capture the velocity magnitude profile well. The *k*-ω and the SST *k*-ω captured the profile better, but did not predict the average value as well as the other models tested. It is for this reason that the SST *k*-ω turbulence model was chosen as the most suitable for analysis of secondary flows, as the flow features are more accurately predicted, thus aiding in understanding secondary flow.

Nomenclature

AGS	Abu-Ghannam and Shaw transition model
k	Turbulent kinetic energy ($m^2.s^2$)
ε	Turbulent energy dissipation rate ($m^2.s^3$)
ω	Specific dissipation rate (s^{-2})
SST	Shear Stress Transport

Introduction

A great deal of research over the years has gone into secondary flows in gas turbine engines, to understand them better. There is yet to be a prediction method that accurately predicts secondary flows [1]. Most of the studies that have been performed have only dealt with experimental investigations of planar or annular cascades, with some studies concentrating on fundamental studies using cylinders [2].

The reason for the popularity of linear cascade studies is due to the reduced complexity. Detailed measurements between the blades are also possible. In an annular, rotating environment it can be prohibitively expensive to perform detailed measurements. For this reason it has become more and more popular to perform numerical studies in place of experimental studies.

Computational Fluid Dynamics (CFD) is currently in common use to analyse turbomachinery due to the significant amount of information that can be obtained. One of the topics of study is the reduction of secondary flows. Reducing the secondary flows reduces the losses and is thus of great interest.

The secondary flow vortex system was first described by Hawthorne [3]. As shown in Figure 1, the passage vortex is the dominant secondary flow feature which has been reported by numerous researchers namely: Marchal and Sieverding[5], Moore and Adhye [6], Moustapha *et al.* [7], Hodson and Dominy [8], and Harrison [9], to name a few. Quoting Gregory-Smith [10], Ingram [11] stated that the passage vortex is formed when a sheared flow is turned. The slower fluid follows a tighter radius of curvature, which leads to the tangential flow across the passage. In order to conserve continuity a vortical flow is generated. The cross passage pressure gradients act to strengthen the passage vortex [12].

Horseshoe vortices are another dominant flow structure. They are caused by the impingement of the boundary layer on the leading edge of the blade, a phenomenon that can also be seen with cylinders [2]. In Figure 2 it can be seen that the horseshoe vortex gets entrained in the passage vortex. Figure 2 was reproduced from Eymann *et al.* [4].

In a rotating environment the inlet flow is skewed as it enters the rotor. As the boundary layer flow enters the rotor, the boundary layer gets skewed due to the change of reference frame caused by the rotating hub. The passage vortex gets further strengthened by this flow [12,14,15,16]. Thus in a rotating environment, like a gas turbine engine, the passage vortex is more pronounced than in a cascade.

Since the secondary flow has a detrimental effect on the performance of the turbine engine, much research has gone into reducing the secondary flows. Some of the methods used include, but are not limited to:

- Blade stacking variations such as the approach of Watanabe and Harada [17].
- Leading edge bulbs and fillets such as the work by Lethander *et al.* [18], and Zess and Thole [19].
- Axisymmetric contouring has been investigated by many authors, for example Boyle *et al.* [20].
- Non-axisymmetric endwall contouring, Gregory-Smith [21], Brennan [22] and Harvey *et al.* [23].

In order to analyse how these reduction mechanisms work, it is necessary to understand how the flow is affected by addition of the mechanism. Numerical analyses are ideal for investigating the flow since all the flow properties are available everywhere in the domain. A suitable turbulence model is required however to capture the flow effects accurately. The current

investigation is aimed at determining which of the turbulence models available in a commercial turbomachinery CFD code; FINE™/Turbo will produce the best results. Once the best turbulence model is determined, it would prove useful in understanding how the previously listed loss reduction mechanisms work.

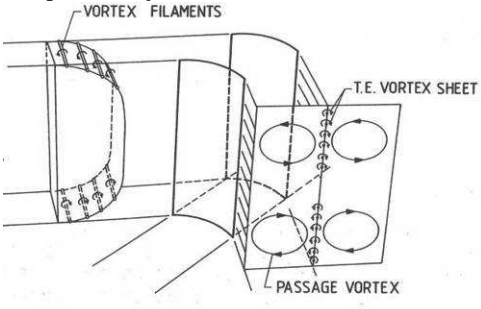

Figure 1: Hawthorne's classical secondary flow model [3]

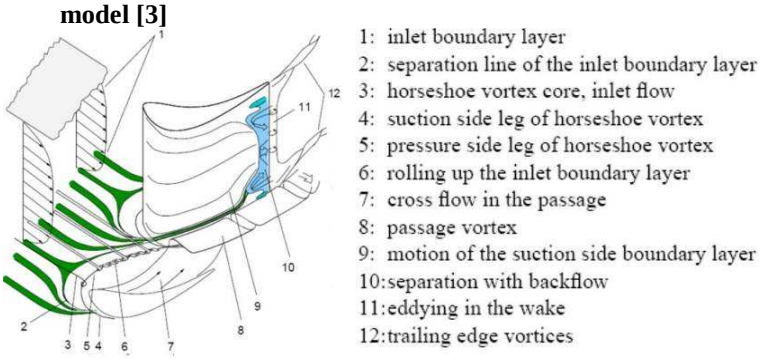

Figure 2: Schematic showing the various vortical structures in a turbine reproduced from Eymann *et al.*[4] who reproduced it from Vogt and Zippel [13].

Experimental setup

The experimental rig used to validate the CFD was described in Snedden *et al.* [24].The instrumentation can be seen in Table 1. The geometry of the blades used was based on the design used in the Durham cascade [25]. The blades were however redesigned such that they would be more appropriate in an annular rotating environment, instead of a linear cascade as originally tested. Thus the blade profile at the hub is the same as in the Durham cascade, but the profile at the tip differs to account for rotation. More about the Durham cascade setup and geometry can be found in Harvey *et al.* [25], Hartland *et al.* [26], Ingram [11] and Snedden *et al.* [24].

Since the measurement is done with a 5 hole probe, profiles of the absolute velocity magnitude will be used for comparison. The measurements downstream of the rotor are averaged because of the rotation and the slow response time inherent in 5 hole probes. Three passes were made downstream of the rotor at different tangential locations so that an average could be taken to minimise the effects of clocking.

Investigation of turbulence models

NUMECA's FINE™/Turbo 7.4.1 CFD package was used for the numerical portion of the current investigation.

Table 1: Experimental instrumentation used by Snedden *et al.* [24]

Primary Instrumentation		
Parameter	**Instrument**	**Uncertainty**
Torque	Himmelstein MCRT 28002T(5-2)CNA-G + Model 721 Mechanical Power Instrument	±0.03N.m
Speed		2RPM
Barometric Pressure	Siemens Sitrans P 7MF4233-1FA10-1AB6-Z A02+B11	0.05% of full scale
Differential Pressure	5 x Siemens Sitrans P 7MF4433-1CA02-1AB6-Z A02+B11	0.05% of full scale
Temperature	PT1000 RTD's	±0.05°C
Secondary Instrumentation		
Steady Flow mapping	Aeroprobe CPC5-C159-305-015.3-16 5 hole cobra probe (1.59mm Ø head)	0.8% in Velocity magnitude, 0.4° in flow angles
Turbulence	TSI 1211-20 single component film	±0.77% mean velocity*
Tangential Traverse	Custom cable system rotating the outer casing	Better than 0.01°
Radial and Yaw traverse	Rotodata Mini actuator	0.01mm 0.1°

*Stamatios (2002)

Numerical boundary conditions

The current steady state investigation is a precursor to future unsteady state research. The unsteady method decided upon was the Domain Scaling method, which is a moving mesh method. Thus the grid used is chosen such that it can be used for steady state as well as unsteady state simulations. To meet the interchangeable criterion the grid had to be created such that the rotor and stator have a matching periodicity. FINE™/Turbo sets this requirement for the Domain Scaling method such that the area of the face upstream of the rotor/stator interface was equal to the face downstream of the interface.

The profiles used to generate the turbine blades can be seen in Figure 3a. The 1½ stage blade assembly used for the CFD analysis can be seen in Figure 3b.

Since the current investigation is interested in the endwall effects, it was considered necessary to have as low a y^+ value as possible. The grid was thus generated with $y^+<2.5$ for the entire endwall and blade surfaces. In order to capture the flow features adequately a fine mesh was used, containing over 5 million cells. This approaches the maximum possible for the available computer, which had 8 gigabytes of RAM.

Turbulence models

The turbulence models investigated were those available in FINE™/Turbo *V*7.4, thus no user coded, or modified turbulence models were investigated. The choice of turbulence models investigated was based on the list of recommended, low Reynolds number models found in the user manual [28] for the flow conditions to be tested. The turbulence models investigated are as follows:

- Baldwin-Lomax
- Spalart-Allmaras
- Spalart-Allmaras with the Abu-Ghannam and Shaw (AGS) transition model
- The low Reynolds number Yang-Shih *k-ε* model
- The non-linear low Reynolds number *k-ω* model
- The Wilcox *k-ω*
- The Shear-Stress Transport (SST) *k-ω*

The Baldwin-Lomax is ideal for design cycle analysis where a robust and fast model is required. It is a two layer algebraic (zero equation) model. The turbulent viscosity is calculated differently in the inner and outer layers. Prantl's mixing length model is used in the inner layer, whereas the mean flow and the length scale are used for the outer layer [28].

The Spalart-Allmaras turbulence model is a one equation model. Unlike the Baldwin-Lomax model, the Spalart-Allmaras model solves the transport equation for eddy viscosity, thus it is always continuous. Due to the robustness and ability to treat complex flows the Spalart-Allmaras has become very popular. Compared to the *k-ε* turbulence model it is more robust and less computationally expensive [28].

The Spalart-Allmaras with AGS is the standard Spalart-Allmaras, with a transition model incorporated in order to determine the transition of the boundary layer from laminar to turbulent. For this investigation only the Abu-Ghannam and Shaw model was investigated, even though other transition techniques are available. The AGS model is based on the correlations obtained by Abu-Ghannam and Shaw [29] obtained using experimental data of transition on a flat plate with pressure gradients [28].

The low Reynolds number Yang-Shih *k-ε* model is a form of the standard *k-ε* turbulence model that does not have a wall function. It infers the boundary layer profile from the input values at the wall [28].

The non-linear low Reynolds number *k-ε* model does not use the first order closure model approximation according to the Boussinesq hypothesis. It is time consuming and is recommended for research only [28].

The Wilcox *k-ω* model [30] predicts free shear flow spreading rates that show good agreement with experiments for far wakes, mixing layers and planar, round and radial jets [28].

The SST *k-ω* model was developed to blend the robustness and accurate formulation of the *k-ω* and the free stream independence of the *k-ε*. The *k-ω* and the *k-ε* are both multiplied by a blending function and added together [31]. The blending function is created such that in the near wall regions the *k-ω* is used, and in the free stream regions, far from the walls, the *k-ε* is used [28,32].

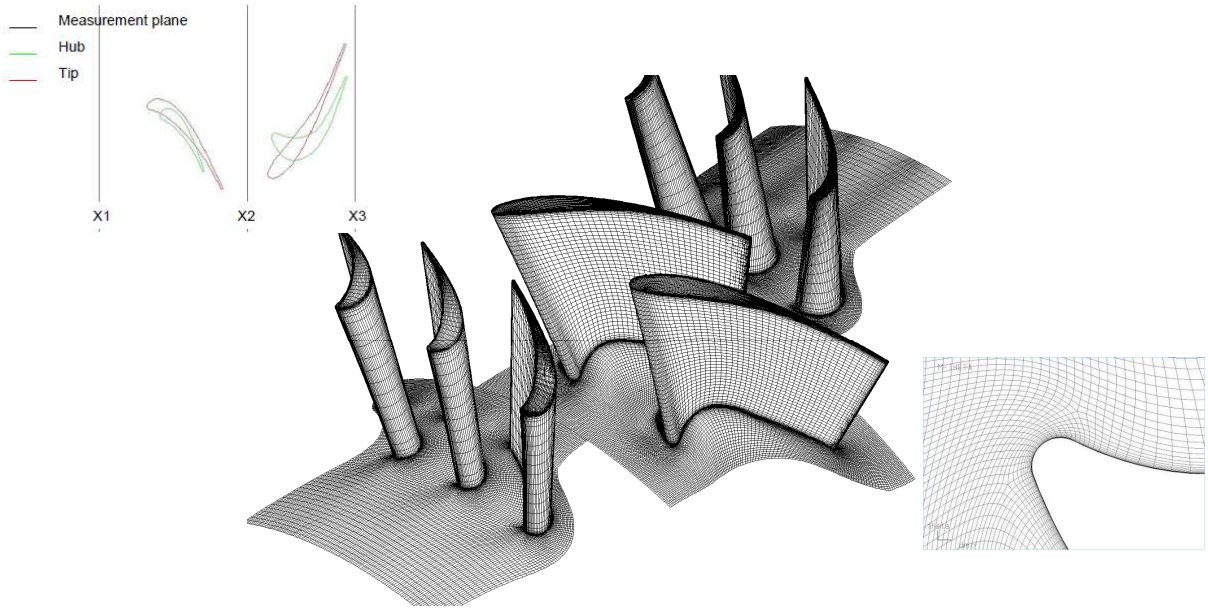

Figure 3: Blade geometry used for the current investigation

Boundary Conditions

The type of boundary conditions that were chosen coincided with the values that were directly measured in the experimental setup of Snedden *et al.* [24], as shown in Table 2. The inlet was specified by velocity components as velocity was the quantity that was controlled in the experiment. The outlet was specified as having a radial pressure equilibrium at midspan (R=0.1725). The working fluid was set as air with perfect gas attributes. The characteristic values listed in Table 2 are used by FINE^{TM}/Turbo to calculate certain values [28].

Table 2: CFD Boundary conditions

Inlet velocity [*m/s*]	21.38
Inlet temperature [*K*]	293
Number of rotor blades	20
Number of stator blades	30
Inlet turbulence [%]	<1
Outlet pressure [*kPa*]	82.9
Rotational speed [*RPM*]	2300
Characteristic length [*m*]	0.06
Characteristic velocity [*m/s*]	25
Characteristic density [kg/m^3]	1.0

Method of comparison

In order to ensure that the turbulence model is appropriate the CFD results will be compared with experimental data. The experimental data used for the comparison was the 5-hole probe steady state measurements. The CFD is therefore run in steady state, using the experimental conditions in order to make an appropriate comparison.

Comparison with pressure plots was not performed because the measurement technique only allowed an approximated static pressure. The 5-hole probe was connected using a modified connection method of Kaiser [33]. The calibration was performed using the method of Ingram [34]. The static pressure is calculated using the pitch ports only, since the yaw ports are only measured relative to each other, allowing a more accurate yaw angle but less accurate static pressure.

Results and Discussion

As can be seen from the list of turbulence models there are some variants. For instance the Spalart-Allmaras model is run with transition modelling and two versions of the k-ε model were tested.

In order to simplify the graphs the variants are compared with each other first. The model that fits the trend best is then compared with all the other turbulence models. By splitting up the comparison in this manner, the number of data series present on the graphs is reduced, making the graphs less cluttered, and easier to interpret. Downstream of the stator there is very little variation in the velocity profile when comparing all the different turbulence models and their variants. Thus none of the variants are plotted in Figure 5a

It was thought that due to the low Reynolds number the flow might be transitional in regions. Thus the inlet turbulence boundary conditions were altered to investigate possible effects of the inlet conditions. For the Spalart-Allmaras three values of turbulence viscosities were used, namely μ_t=0.0001, μ_t=0.0005 and μ_t=0.0009. The default value in FINE^{TM}/Turbo is μ_t=0.0001 and is typical for external flows [28]. For turbo-machinery flows the recommended value of turbulence viscosity is between μ/μ_t=1 and μ/μ_t=5, thus the extreme values as well as a middle value is chosen (these values are based on the viscosity of air as being μ=1.8e^{-5}Pa.s).

Comparison of variants

Looking at Figure 4a and Figure 4b it is evident that there is negligible difference between the different variants, even when changing the inlet turbulence level. Changing the turbulent viscosity level any more increases it beyond the recommended levels [28], thus ratios beyond this limit were not tested. Figure 4a shows that the predicted values were at the appropriate level.

The experimental average velocity is v=24.92m/s compared to the numerical average velocity of v=24.79m/s. The trend is approximately correct, but it does not capture all features in the profile. Since all the variants of the Spalart-Allmaras produce approximately the same velocity profile, only the standard Spalart-Allmaras will be compared with the other turbulence models, due to its reduced computational expense.

The biggest differences between the experimental results and the numerical results are found at the hub and casing. Since the resolution in the experimental measurements at the hub and casing are not as fine as the numerical results, the differences in turbulence models in this region are not relevant.

As with the Spalart-Allmaras, the k-ε variants are very similar. To reduce complexity the Yang-Shih k-ε turbulence model is thus treated as the best, since the added complexity of the variants do not improve the accuracy.

The k-ω variants are significantly different, and are thus compared directly with the other turbulence models.

Comparison of turbulence models

With the differences in the turbulence model variants known it is now possible to find which turbulence model produces the best correlation. Looking at Figure 5a it is evident that none of the turbulence models show an ideal correlation. The turbulence models either have a good area averaged velocity, or a good reproduction of the velocity profile. A good reproduction of the velocity profile is sought, since the current investigation is more interested with flow features and not mean values.

Figure 5 shows that all the turbulence models produce very similar results. At the casing, however the correlation is not as good as at the hub. The low value of

the point R=0.196m in the experimental velocity profile is thought to be due to the tip leakage flow. It is thought that the over-prediction of the velocity at the casing is due to manufacturing anomalies in the experimental setup. The tip gap could be slightly larger then predicted, either due to a blade being slightly shorter or due to the casing not being perfectly circular at the measurement locations. Some of the discrepancy could also be attributed to the hole through which the probe is inserted into the flow.

With reference to Figure 5b it is clear that all the turbulence models fail in some aspect or another. The Spalart-Allmaras, Baldwin-Lomax and the k-ε follow the values at an appropriate level, but do not capture the profile very well. The k-ω and the SST k-ω however follow the profile reasonably well, but fail to capture the correct values.

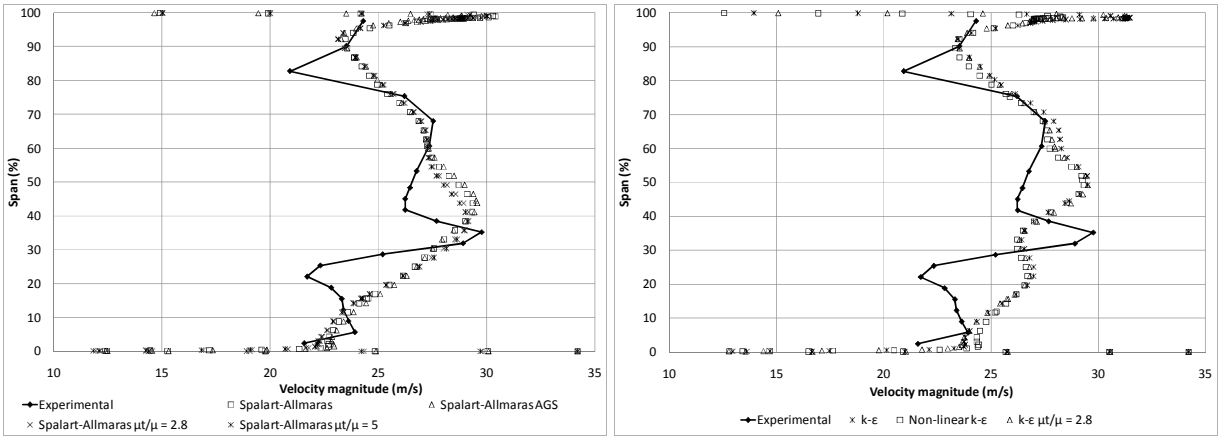

Figure 4: Comparison of the numerical and experimental contour plot downstream of the rotor

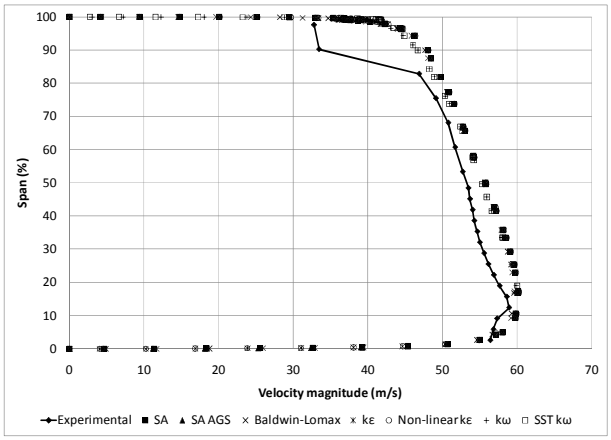

(a) Effect of the turbulence models on velocity magnitude downstream of the stator

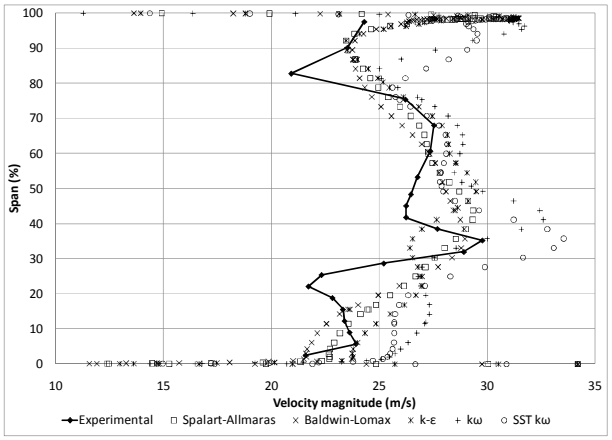

(b) Effect of the turbulence models on velocity magnitude downstream of the rotor

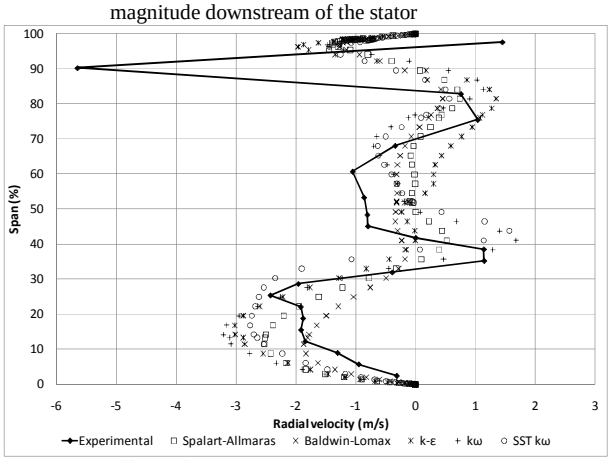

(c) Effect of the turbulence models on radial velocity downstream of the rotor

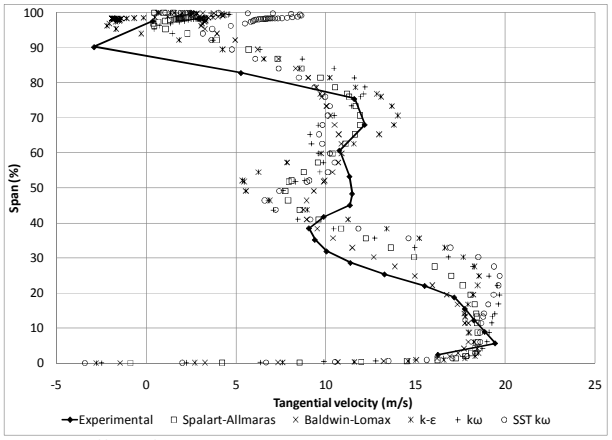

(d) Effect of the turbulence models on tangential velocity downstream of the rotor

Figure 5: Comparison of the numerical and experimental contour plot downstream of the stator (a) and rotor (b,c,d)

In the current investigation the trend is of more importance then the actual values, since the values can generally be captured experimentally. The trend is a result of the flow features, these features and the manner and location in which they are initiated are of importance, since this aids in understanding of the flow features. Thus the *k-ω* models are the most appropriate.

The Wilcox *k-ω* [30] captures the trend very well at the casing, with the tip leakage flows peaking in the same locations. Conversely at the hub it does not quite capture the position of the peaks. The trend shows the correct type of features, but in the wrong locations. The SST *k-ω* however captures the hub features very well, but captures the flow features poorly at the casing. Therefore the SST *k-ω* was chosen, since the area of interest is the flow near the end wall.

Conclusions and Recommendations

Looking at the velocity profiles it was evident that none of the current turbulence models were sufficient to model the secondary flows present in a rotating environment. Thus the most appropriate turbulence model was determined from a set of available turbulence models in a commercial CFD code, Numeca's FINE^{TM}/Turbo. It was found that the Spalart-Allmaras and the Baldwin-Lomax models are adequate for the cases where the average velocity, and thus flow rates are of importance. The Spalart-Allmaras and the Baldwin-Lomax models also have a lower computational expense then the other models.

The *k-ε* models gave a fair approximation, but did not improve the accuracy of the simulation when compared to the added computational expense. The *SST k-ω* model performed the best out of the two *k-ω* models tested. It did not capture the velocity values very accurately, but it captured the velocity magnitude profile the best of all the turbulence models tested.

With reference to the data it is evident that Baldwin-Lomax is still one of the best all purpose models for turbomachinery. The *SST k-ω* shows some promise as it predicted the velocity magnitude reasonably well, but the Baldwin-Lomax predicted the radial and tangential velocities better.

Due to the complex nature of secondary flow it may still be sometime before computational hardware and the numerical models are such that the complexities can be appropriately modelled. Until such time it is important that new models be investigated and validated against experimental data. It is also recommended that the computational expense be carefully weighed against the required accuracy. FINE^{TM}/Turbo does offer higher order turbulence models, but they are non-linear and not recommended for use in design cycle analysis [28] due to the added computational expense.

Acknowledgments

The authors would like to gratefully acknowledge Project VITAL and the CSIR for financial support, without which none of the current research would have been possible.

References

[1] LS Langston. *Secondary flows in axial turbines - a review.* Heat Transfer in Gas Turbine Systems Annals of the N.Y.Academy of Sciences, 2001.

[2] L Belik. *The secondary flow about circular cylinders mounted normal to a flat plate.* Aeronautical Quarterly, pages 47–54, 1972.

[3] W.R. Hawthorne. *Rotational flow through cascades.* Journal of Mechanical and Applied Mathematics, 3, 1955.

[4] S Eymann, U Reinmoller, R Niehuis, W Forster, Beversdorff M, and J Gier. *Improving 3D flow characteristics in a multistage lp turbine by means of endwall contouring and airfoil design modification - part 1: Design and experimental investigation.* ASME TURBO EXPO GT-2002-30352, 2002.

[5] P Marchal and CH Sieverding. *Secondary flows within turbomachine bladings.* In Secondary flows in turbomachines, volume AGARD-CP-214 Paper 11, 1977.

[6] JG Moore. *Calculation of 3D flow without numerical mixing.* pages 8.1–8.15. AGARD-LS-140 3D Computational Techniques applied to Internal Flows in Propulsion Systems, 1985.

[7] SH Moustapha, GJ Paron, and JHT Wade. *Secondary flows in cascades of highly loaded turbine blades.* Transactions of ASME Journal of Engineering for Gas Turbines and Power, 107:1031–1038, 1985.

[8] HP Hodson and RG Dominy. *The off-design performance of a low-pressure turbine cascade.* Transaction of the ASME Journal of Turbomachinery, 109:201–209, April 1987.

[9] S Harrison. *Secondary loss generation in a linear cascade of high-turning turbine blades.* Transactions of ASME Journal of Turbomachinery, 112:618–624, 1990.

[10] D. Gregory-Smith. *Lecture 1: Physics of secondary flows lecture 2: Sec- ondary flows and vorticity lecture 3: Secondary loss: Loss generation, effect of blade design, loss correlations and modelling.* von Karman Institute for Fluid Mechanics, 1997. Secondary and Tip Clearance Flows in Axial Turbines.

[11] GL Ingram. Endwall *Profiling for the Reduction of Secondary Flow in Turbines.* PhD thesis, University of Durham, July 2003.

[12] JP Bindon. *The effect of hub inlet boundary layer skewing on the endwall shear flow in an annular turbine cascade.* In ASME 79-GT-13, ASME 79-GT-13, 1979.

[13] H.F. Vogt and M. Zippel. *Sekundarstromungen in turbinengittern mit geraden und gekrummten schaufeln; visualisierung im ebenen wasserkanal.* Forschung im Ingenieurwesen, Engineering Research, 62 no. 9:247 – 253, 1996.

[14] JP Bindon. *Exit plane and suction surface flows in an annular turbine cascade with a skewed inlet*

boundary layer. International Journal of Heat and Fluid Flow, 2 No. 2:57–66, 1980.

[15] E Boletis, CH Sieverding, and W Van Hove. *Effects of skewed inlet endwall boundary layer on the three dimensional flow field of an annular turbine cascade.* AGARD CP351 Paper 16, 1983.

[16] JA Walsh and D Gregory-Smith. *The effect of inlet skew on the secondary flow and losses in a turbine cascade.* In Proceedings of the Institute of Mechanical Engineering International Conference - Turbomachinery Efficiency Prediction and Improvement, pages 15–28, 1987.

[17] H Watanabe and H Harada. *Suppression of secondary flows in turbine nozzle with controlled stacking shape and exit circulation by 3D inverse design method.* ASME 99-GT-72, 1999.

[18] AT Lethander, KA Thole, GA Zess, and J Wagner. *Optimizing the vane-endwall junction to reduce adiabatic wall temperatures in a turbine vane passage.* ASME International Gas Turbine Institute Turbo Expo, 5:711–721, 2003.

[19] GA Zess and KA Thole. *Computational design and experimental evaluation of using a leading edge fillet on a gas turbine vane.* Transactions of ASME Journal of Turbomachinery, 124:167–175, 2002.

[20] RJ Boyle, HE Rholik, and LJ Goldman. *Analytic investigation of effect of end-wall contouring on stator performance.* Technical report, 1981.

[21] D Gregory-Smith. 3D *flow simulation in turbomachinery - the ercoftac seminar and workshop ii* January 1994. pages 35–49. VDI Berichte No. 1185, 1995.

[22] G Brennan, N Harvey, MG Rose, N Fomison, and MD Taylor. *Improving the efficiency of the trent 500 hp turbine using non-axisymmetric end walls: Part 1 turbine design.* In ASME TURBO EXPO 2001, ASME 2001-GT-0444, 2001.

[23] N Harvey, G Brennan, DA Newman, and MG Rose. *Improving turbine efficiency using non-axisymmetric endwalls: Validation in the multi-row environment and with low aspect ratio blading.* In ASME TURBO EXPO 2002, ASME 2002-GT-30337, 2002.

[24] Glen Snedden, Thomas Roos, Dwain Dunn, and David Gregory-Smith. *Characterisation of a refurbished 1Â½ stage turbine test rig for flow field mapping behind blading with non-axisymmetric contoured endwalls.* In ISABE, number ISABE 2007-1363, 2007.

[25] N Harvey and K Ramsden. *A computational study of a novel turbine rotor partial shroud.* In ASME Turbo Expo 2000 Paper 2000-GT-668, pages –, 2000.

[26] J Hartland, D Gregory-Smith, N Harvey, and MG Rose. *Non-axisymmetric turbine end wall design: Part ii experimental validation.* ASME 99-GT-338, 1999.

[27] Numeca International. Numeca brochure. http://www.numeca.com/fileadmin/user_upload/numeca_brochure_01.pdf, August 2008.

[28] Numeca International, 5, Avenue Franklin Roosevelt, 1050 Brussels, Belgium. User Manual FINE™Turbo v8 (including Euranus) Documentation v8a, v8a edition, October 2007.

[29] Shaw R. Abu-Ghannam BJ. *Natural transition of boundary layer - the effect of turbulence, pressure gradient and flow history.* Journal of Mechanical Engineering Science, 22 (5):213–228, 1980.

[30] D.C. Wilcox. *Turbulence Modeling for CFD.* DCW Industries, Inc., La Canada, California, 1998.

[31] F. R. Menter. Two-*equation eddy-viscosity turbulence models for engineering applications.* AIAA Journal, 32:269–289, 1994.

[32] D.I. Dunn. The *numerical investigation of a bank of delta plenum air-cooled heat exchangers.* Master's thesis, University of Cape Town, 2006.

[33] I Kaiser. *The effect of tip clearance and tip gap geometry on the performance of a one and a half stage axial gas turbine*. PhD thesis, 1996.

[34] G Ingram and D Gregory-Smith. *An automated instrumentation system for flow and loss measurements in a cascade.* Flow Measurement and Instrumentation, 2005.